



# Assessment of noise attenuating powertrain components

Karina Windhofer<sup>1</sup> · Alexander Kari<sup>1</sup> · Klaus Prenninger<sup>1</sup> · Stephan Lange<sup>1</sup>

Received: 4 December 2020 / Accepted: 16 February 2021  
© Springer-Verlag GmbH Deutschland, ein Teil von Springer Nature 2021

## Abstract

Wind turbine noise used to be dominated by aerodynamic blade noise, effectively masking mechanical noise, originating from the drivetrain. Successful blade noise reduction makes mechanical noise audible. Resonances can cause annoying tonalities which hardly can be avoided with standard measures. The basic idea is to get down to the root cause of the problem: Excitations are being mitigated at its source in order to avoid the formation of structure born sound, rather than trying to dampen the propagation of noise at any location of the transfer path through the drivetrain structure. Powertrain components (torsional dampers and torsional elastic couplings) used for many decades to reduce torsional vibrations of combustion engines, are also being applied since a while to reduce mechanical engine noise, by dampening torsional vibrations of the camshaft caused by excitations of the injection pump [1]. An assessment of such technologies integrated to a wind gearbox by applying torsional vibration calculations (TVC) is main objective of this paper.

## Bewertung Körperschallmindernder Triebstrangkomponenten

### Zusammenfassung

Lange wurden Schallemissionen von Windturbinen durch aerodynamische Blattgeräusche bestimmt. Diese überdeckten recht wirkungsvoll den vom Triebstrang kommenden mechanischen Körperschall. Die Reduktion von Blattgeräuschen lässt mechanische Geräusche hörbar werden. Resonanzen können zu unangenehmen, hörbaren Tönen führen, welche durch Standardmaßnahmen in Zukunft nur mehr schwer vermieden werden können. Die grundsätzliche Herangehensweise dieser Arbeit besteht darin, das Problem an der Wurzel zu anzugehen: Das Bedämpfen der Anregungen an Ihrem Ursprung, um die Bildung unzulässigen Körperschalls zu vermeiden, anstatt die Schallausbreitung entlang der Struktur des Triebstranges zu mindern. Triebstrangkomponenten, im vorliegenden Fall Drehschwingungsdämpfer und drehelastische Kupplungen, werden seit Jahrzehnten erfolgreich eingesetzt um Drehschwingungen an Verbrennungskraftmaschinen zu reduzieren. Diese finden auch als Körperschallmindernde Maßnahme im Rädertrieb von Motoren Verwendung, um die durch Anregungen der Einspritzpumpe verursachten Drehschwingungen, und dem daraus resultierende Körperschall, effektiv zu bedämpfen [1]. Eine Bewertung derartiger, getriebeintegrierter Lösungen durch Anwendung von Drehschwingungsmodellen, auch TVC genannt (torsional vibration calculation), ist Hauptgegenstand dieser Arbeit.

## 1 Introduction

Regulations of noise emittance of European onshore wind parks not only become more stringent: Many national regulations for operating wind turbines contain a penalty for wind farm noise with one or more tones [1]. Growing size of structures of wind turbines and the need for energy produc-

tion at low wind speeds, but also during night, might lead to an increasing demand on mitigations to avoid tonalities and reduce the overall noise of wind turbines. As a result of the enormous progress in blade aerodynamics during recent years, the sound power level of blades diminished gradually. The reduction of the masking energy very likely makes mechanical noise audible. Noise originating from the drivetrain, mainly resulting in tonalities and low-frequency noise, propagates through the entire drivetrain structure and radiates through the blades, the tower, and the nacelle housing [2]. All considered, it is self-evident that wind turbine and gearbox manufacturers will have to investigate in new

✉ Alexander Kari  
lncs@springer.com

<sup>1</sup> Geislinger GmbH, 5300 Hallwang, Austria

technologies to avoid tonalities and noise radiation, in order to cope with future regulations and to grow energy yield also in urbanized areas.

This paper shows how powertrain components get back to the root cause of the problem: Excitations are being mitigated at its source to avoid the formation of structure born sound, rather than trying to dampen the transfer of noise at any location of the transfer path throughout the drivetrain structure. In wind turbines, one of the main sources of drivetrain noise is the excitation caused by gear mesh in the second planetary stage. This torsional excitation entails the planetary carrier in resonance with the gearbox housing, inducing torsional vibrations to the entire drivetrain. This study only covers the possibility to reduce these vibrations by torsional dampers and torsional elastic couplings, which are described in detail under Sect. 3.2.

The introduction part covers a short insight to torsional vibrations of internal combustion engines, a cross-reference to the application and experience with noise attenuating powertrain components in gear drives of engines. Followed by an overview on powertrain components (torsional vibration damper technologies, torsional elastic coupling), describing its general setup and mode of operation including its possible use in a wind gearbox.

The two main parts of this paper describe the assembly of the simulation model used, and the assumptions taken, followed by describing simulation results (frequency of various options) in terms of combination of different powertrain components and locations in the gearbox.

The introduction part covers a short insight to torsional vibrations of internal combustion engines, a cross-reference to the application and experience with noise attenuating powertrain components in gear drives of engines. Followed by an overview on powertrain components (torsional vibration damper technologies, torsional elastic coupling), de-

scribing its general setup and mode of operation including its possible use in a wind gearbox.

The two main parts of this paper describe the assembly of the simulation model used, and the assumptions taken, followed by describing simulation results (frequency of various options) in terms of combination of different powertrain components and locations in the gearbox.

## 2 Torsional vibrations

### 2.1 Internal combustion engines

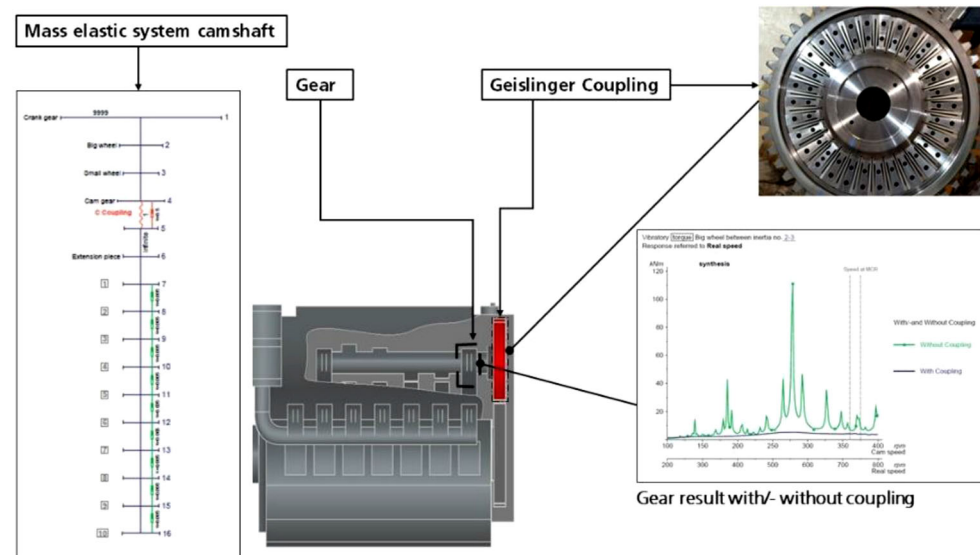
Combustion cycles in combination with mass moments of inertia and elastic drivetrain components are causing severe torsional excitations in internal combustion engines, resulting in high dynamic loads and stresses of the crankshaft and the overall powertrain. To reduce stress levels and to safeguard these components also under severe operating conditions, such as one-cylinder-misfiring, the use of torsional vibration dampers and couplings in large combustion engines is state-of-the-art since many decades [3].

### 2.2 Mechanical engine noise

In large diesel engines most of the engine noise stems from mechanical excitations rather than combustion noise [4]. Torsional vibrations of the camshaft are caused by excitations of the injection pump, leading to gear teeth impact in the gear train between crankshaft and camshaft. The generated energy is transferred through the camshaft bearings to the engine structure which radiates noise.

Acoustic tiles on the walls of the engine room and engine covers certainly reduce noise to meet regulations. However, additional costs arise, and engine covers complicate servic-

**Fig. 1** Simulation of a camshaft coupling in a gear train



ing work. Other than isolation material, a torsional vibration damper or a torsional elastic coupling gets down to the root of the problem. Excitations are being mitigated to avoid the formation of structure born sound instead of trying to reduce noise after it has been created (see Fig. 1).

The design and the effect of various technologies for torsional vibration mitigation, which are the matter of investigations in this paper, are described in the following section.

### 2.3 Application of torsional dampers and torsional elastic couplings

In drivetrains torsional vibrations occur when torsional excitations match with torsional eigenfrequencies, resulting in unfavorable effects, such as impermissible component stress levels or increased structure borne sound. To mitigate these effects, additional elements like tuning masses, torsional dampers and torsional elastic couplings can be added to the system.

A torsional damper is an additional component consisting of a tuning mass coupled with a defined torsional stiffness and damping to a primary mass which is rigidly attached to the drivetrain. These dampers are most effective, when installed at, or close to a location, where the eigenform has a significant amplitude.

Other than a torsional damper, a torsional elastic coupling is integrated to the torque path of a drivetrain and adds additional elasticity to the torsional system. A new

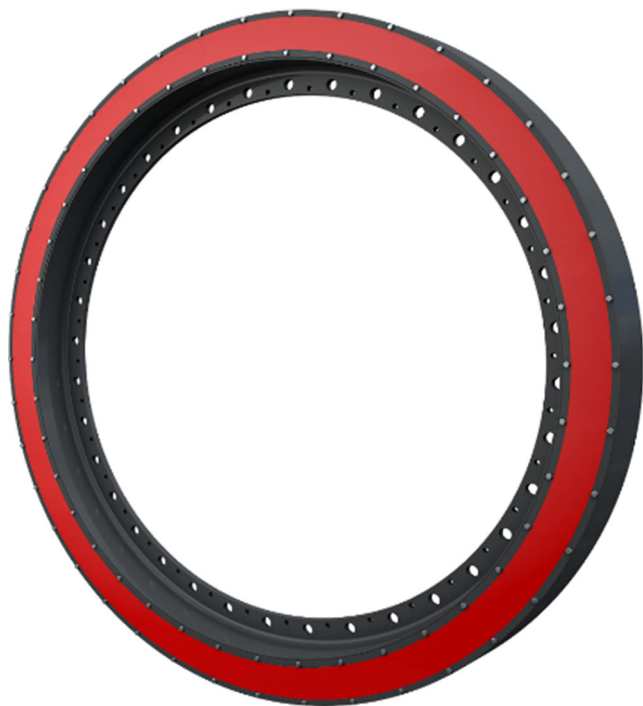


Fig. 2 Geislinger Vdamp® viscous type damper [5]

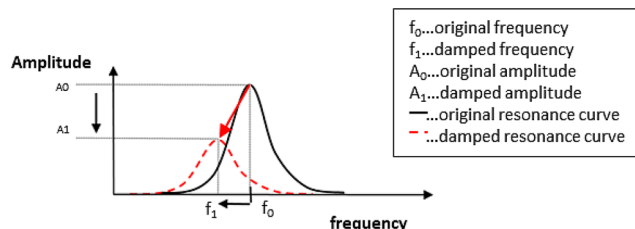


Fig. 3 Illustration of amplitude damping effect of a viscous damper

first eigenfrequency is introduced; the torsional elastic system is split up into two sub-systems, each vibrating at reduced magnitudes with the coupling as the twisting element in between. Two important characteristics are to be considered: First, the higher the torsional elasticity of the coupling is, the lower the new eigenfrequency is. Second, the bigger the difference is between excitation frequency and the new eigenfrequency, the more effectively the coupling isolates the two sub-systems from excitations and acts as a low-pass filter. Torsional elastic couplings can also add additional relative damping to reduce low frequency amplitudes and to limit coupling twist.

### 2.4 Torsional viscous damper

A viscous type damper basically consists of a housing with an inertia ring which is coupled to the housing by a special, high-viscous silicone oil (see Fig. 2). Torsional vibrations result in an angular offset between damper housing and inertia ring. This applies shear load to the silicone oil, converting the vibration energy into heat and transferring it to the ambient. Vibration amplitudes are effectively mitigated over a wide frequency spectrum. Silicone oil as a viscos-elastic material has elastic and damping properties, both depending non-linear on temperature and vibration frequency. By selecting the oil viscosity from a range of available products and designing the dimensions of the internal shear gaps, the damper can be tuned to achieve a maximum damping effect to the drivetrain.

Fig. 3 describes the effect of the viscous damper on the torsional system. The black graph represents the original resonance of the system. A viscous damper reduces vibration amplitudes  $A_0$ – $A_1$  and resonance frequency  $f_0$  is shifted down to  $f_1$ .

The damping effect is a result of shear damping between housing and inertia ring of the silicone oil. The frequency shifting effect is a result of adding housing inertia and, because coupled by the silicone oil, also a part of the inertia ring. The magnitude of contribution to resonance frequency shifting by the inertia ring also depends on the damper tuning: The higher the oil viscosity is and the smaller the gap is, the larger the effect.



Fig. 4 Steel spring damper [5]

Normally, a viscous damper reduces crankshaft stresses in combustion engines or protects the shaft line between the engine and the propeller. In a wind gearbox, a viscous damper attenuates the torsional mode, where the second stage planetary carrier is in resonance with the gearbox. It mitigates amplitudes at the source of origin. This type of damper is rather flexible in terms of installation space.

The challenge in performing torsional vibration analysis is to consider the non-linear stiffness and damping proper-

ties and its temperature dependency due to the non-linear characteristics of the silicone oil. Analysis over the entire frequency range requires amplitude calculations at various stiffness—damping combinations and consolidating results in one plot [3, 6].

## 2.5 Torsional steel spring damper

Fig. 4 shows an all-steel tuned mass damper with radially arranged, fatigue-resistant spring blades, which are widely used as crankshaft dampers in large combustion engines. Like a viscous damper, it protects the entire driveline from the crankshaft to the propeller and reduces the overall crankshaft stress level.

The diagram below describes how the damper works (see Fig. 5.). The first picture shows the vibration amplitude without a damper. The second picture illustrates how the stiffness ( $= c$ ) added to the system by means of the spring blades splits the resonance frequency into two new ones, one at lower, one at higher frequency. Adding optimal relative damping ( $= d_r$ ) to the system the damper further reduces the amplitude of the two remaining resonances, achieving optimal reduction for lowest structural vibrations.

The overall damping effect is a combination of friction and hydrodynamic damping and is illustrated in Fig. 6. friction damping stems from friction between the spring blades and friction between the spring blade tips and the grooves of the inner damper member. The design of the damper which cavities are filled with oil allows additional hydrodynamic damping. Torsional vibrations lead to an offset between the outer and the inner damper member, oil is forced to flow from cavity A to cavity B trough the radial restriction between the coupling members.

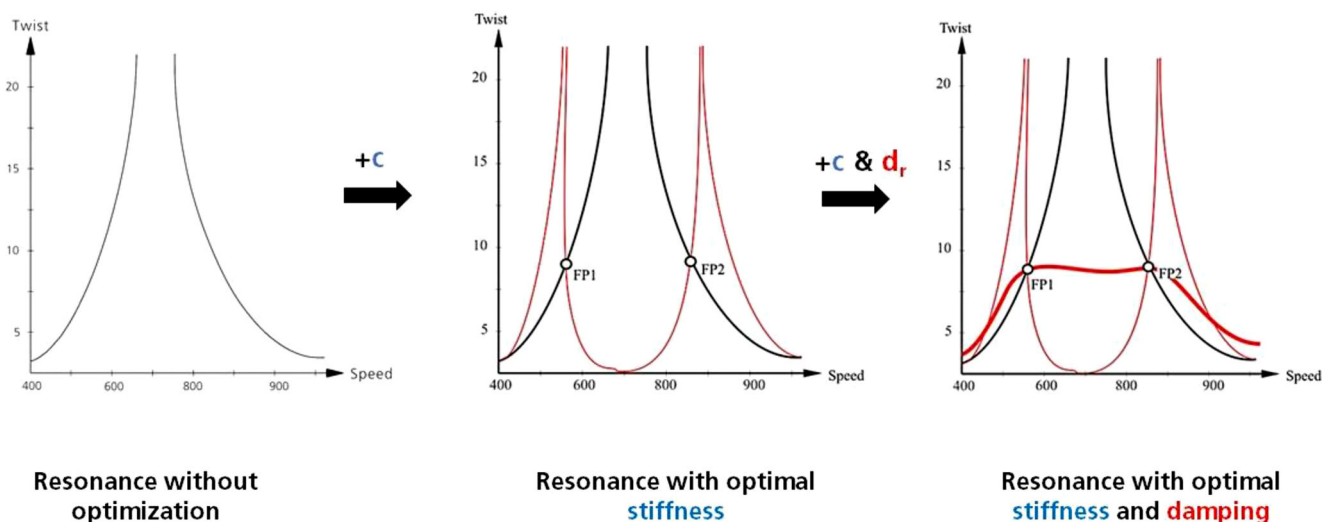
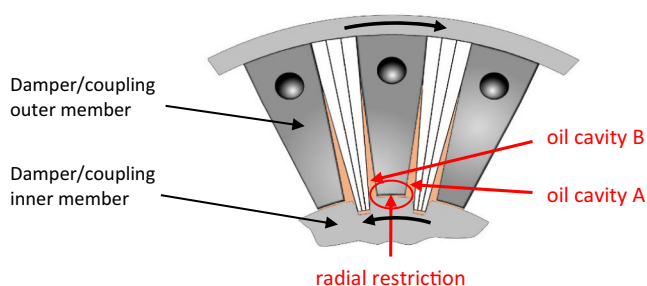


Fig. 5 Functionality diagram of a spring type damper



**Fig. 6** Friction and hydrodynamic damping of spring type damper and coupling

The damping of a torsional elastic coupling described hereinafter under 2.6 works according to the same principal. To avoid undesirable cavitation, pressurized oil supply is required.

The challenge of applying a steel spring damper to a wind gearbox is to find sufficient installation space close to the source of excitations. The tuning of the steel spring damper to such a high main resonance requires a high torsional stiffness with a relatively low inertia. Based on these two parameters the damping value can be calculated [3, 6].

## 2.6 Torsional elastic coupling

Like the steel spring damper, the coupling is a robust all-steel product with tunable mechanical stiffness and hydrodynamic damping (Fig. 7). The difference is that the coupling is transmitting static torque: additionally, other than a damper, a coupling is separating the torsional system into two tuned subsystems by introducing elasticity to the torque path. For this reason, vibratory torques can hardly be transmitted. Vibrations are diminished, and the noise transfer is attenuated significantly. The damping properties of the coupling further reduce the resonance amplitudes.

An elastic coupling can be placed to the torque path between the first and second planetary stage, but also integrated to the gearwheel of the parallel stage (for three-staged gearboxes only), similar to a camshaft coupling (see Fig. 1). The first option is highly effective but requires a large installation space and, because of the enormous torque, it will result in a comparatively big and heavy coupling. The identification of further possible positive effects on drivetrain dynamics are not subject of these investigations. Integrated to the parallel stage, this option is obviously not requiring additional installation space. For both options, considerably high axial loads because of the helix gear angle need to be considered and should be absorbed by the coupling [7].



**Fig. 7** Torsional elastic coupling [5]

## 3 Simulation model

### 3.1 Model design

For steady state calculations inhouse developed software is used. GTVC (Geislinger Torsional Vibration Calculation) is based on a vast experience of many years, known as a reliable tool for simulations of the torsional system of combustion engines. For torsional vibration calculations, two basic concepts of analysis are available, steady state analysis and transient analysis.

To achieve profound results, it is decided that transient analysis is applied for this study. For this reason, a software capable of transient calculations is applied. In a first step, the complex gearbox model is transferred into a simplified model. Original equipment manufacturer's data are reduced to a minimum. An additional advantage is reduced computation time. Fig. 8 shows the complex mode (top) and the simplified model (bottom).

First complexity reduction is achieved by simplifying the planet gears, i.e. dividing into their individual gear ratios: The gear ratio between ring gear and planet gears and the ratio between planet gears and sun gear. After the subdivision into the individual translations, the inertias of the planet gear are merged into a single inertia. Based on the paral-

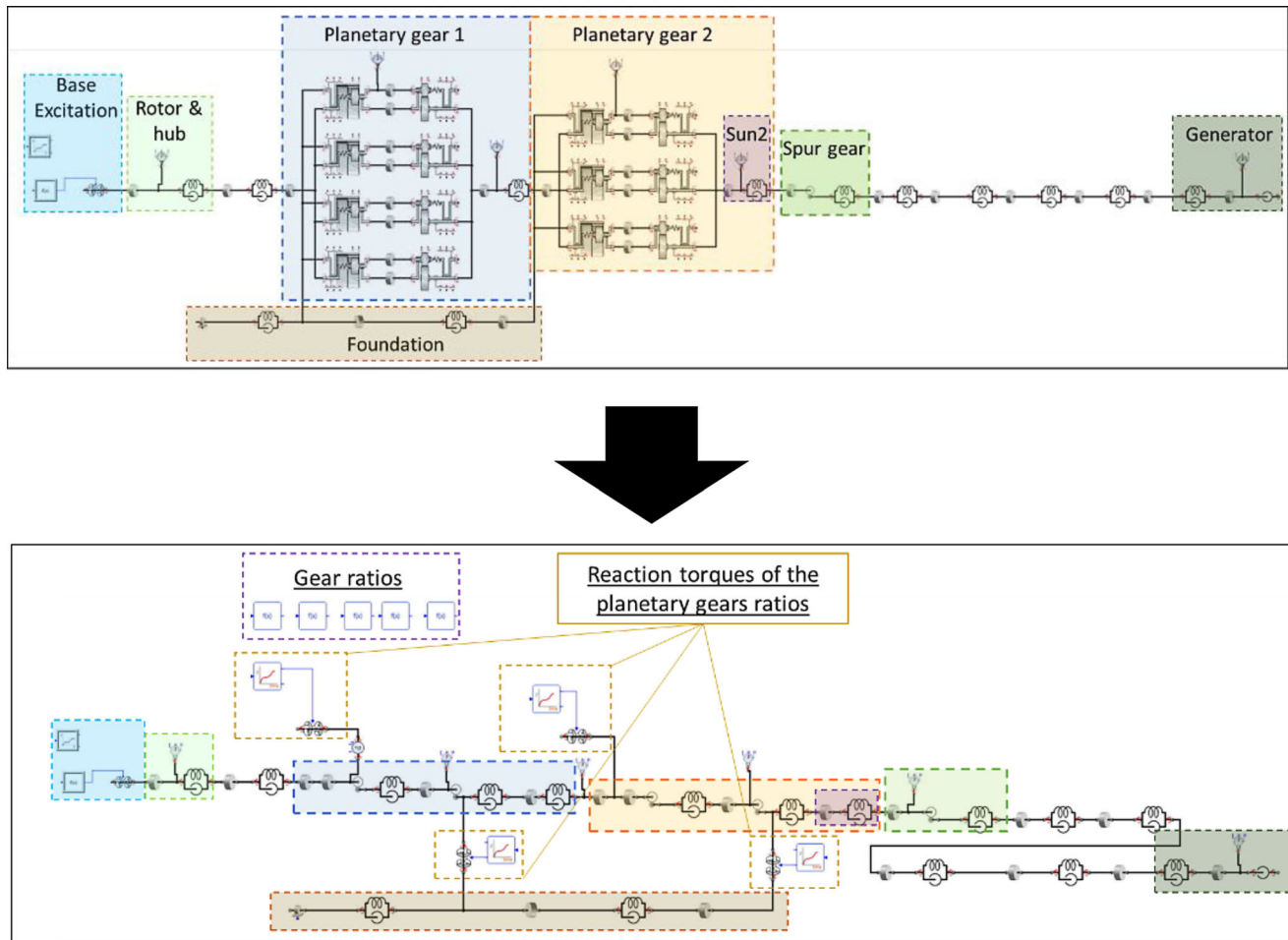


**Fig. 8** Detailed model (*top*) and simplified model (*bottom*) of a three-stepped gearbox (Simulation-X)

parallel axis theorem, there are additional inertias for the other planet gears. These inertias are also merged into one inertia. One must pay attention to the translation because the planetary inertia already takes effect after the translation, but their additional inertia, results from parallel axis theorem, runs at the same speed as the planet carrier. This means that theoretically the inertia of the planet carrier with the resulting inertia from the parallel axis theorem can also be combined into one inertia. The stiffnesses are also reduced to a single value. The challenge with gearboxes is the fluctuation of the tooth stiffnesses, i.e. it cannot be represented by a normal stiffness element. The stiffness is described by two parts to achieve a better approximation. According to literature, the stiffness of a gear consists of the proportion of the static stiffness and the proportion of the dynamic stiffness [8]:

$$k(\varphi) = k_{st} + k_{dyn}F(z\varphi) \quad (1)$$

The part  $F(z\varphi)$  describes the periodical function over the angle and tooth  $z\varphi$ . Using this approach, the static stiff-

ness is mapped with a normal stiffness element using the following equation [8]:

$$k_{st} = \frac{\bar{k} \cdot \left(\frac{d_0}{2}\right)^2 \cdot b}{\cos \beta}, \quad (2)$$

Whereas  $\bar{k}$  is the specific stiffness,  $d_0$  is the pitch circle diameter,  $b$  is the width of the gear and  $\beta$  is the helix angle of the toothing. In this model, the dynamic stiffness is not mapped as stiffness, but inserted in as a reaction torque. This means in addition to the classically requested mass elastic data (inertia, stiffness, damping, etc.), and the reaction torques generated in the planetary gear are needed. Occurring forces generate moments through the tooth stiffness fluctuations. Therefore, the gear mesh excitation can be mapped to the simplified model by means of the reaction torques (see Fig. 9).

For a first evaluation of potential options further assumptions are made to keep the computation time short. The 4+ Megawatt class wind turbine drivetrain investigated with its three-stepped gearbox is described by the detailed model il-

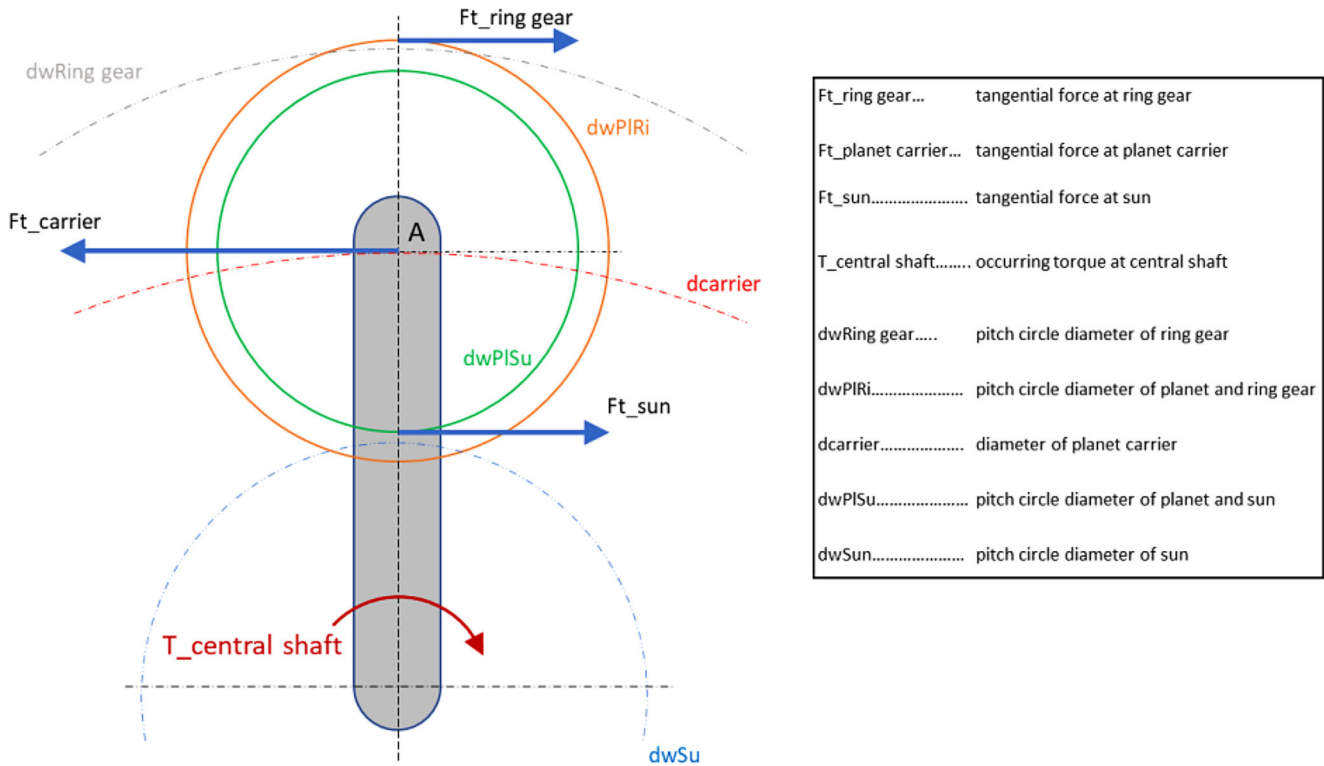


Fig. 9 Occurring reaction forces and torques

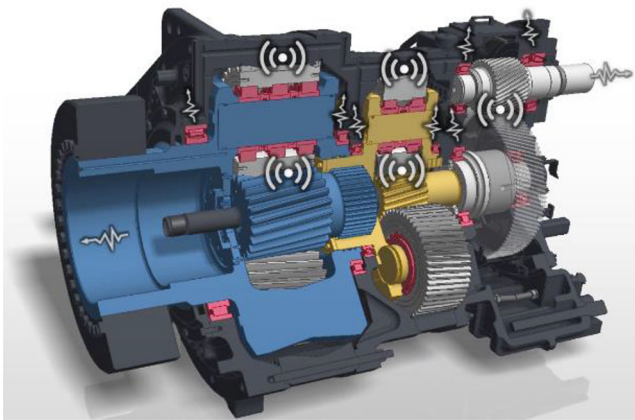


Fig. 10 Three-stepped gearbox indicating sources of noise emissions [9, p. 120]

illustrated by Fig. 8. A tooth stiffness variation of  $\pm 5\%$  in both planetary gears is taken as a conservative approach recommended by a wind gear box manufacturer. Rotor and hub are modeled as simplified rigid inertias. A constant torque is applied as basic excitation, at which a first harmonic oscillation was superimposed by a sine curve of  $\pm 2.5\%$  of torque.

### 3.2 Options investigated

Fig. 10 illustrates the sources of noise emissions in a three-stepped gearbox. The main sources are the gear meshing, mainly where the tooth flanks of the planet gears of the second stage are in engagement with the ring gear. That induces a torsional mode where the second planetary carrier is in resonance with the gearbox housing. The major resonance amplitude is mainly in a frequency range between 140 and 160 Hz.

Due to the complexity of the problem and the myriad of possibilities, this study focuses on five different options of noise attenuating solutions (viscous damper, steel spring damper, elastic coupling) in different locations in a three-stepped gearbox (see Fig. 11 and Table 1).

## 4 Results

Table 2 shows the comparison between the eigenfrequencies of the different models, for the complex model, and for the simplified model (Fig. 7). Except the first eigenfrequency, deviations are below 5%, which can be considered as precise enough for an initial assessment of the mode of action in this study.

The focus of evaluations is on the torque of the second stage sun wheel, referred to as “sun2”. Sun2 is also

**Table 1** Description of potential options

| Option | Description  |
|--------|--|
| 1      | Elastic coupling in the torque path between 1st and 2nd planetary stage                |
| 2      | Steel spring damper attached to 2nd planetary stage, rotor side                        |
| 3      | Viscous damper attached to 2nd planetary stage, between planet carrier and gear wheels |
| 4      | Elastic coupling in the torque path sun shaft and 3rd stage; gear integrated           |
| 5      | Steel spring damper attached to the spur gear wheel of the 3rd stage                   |

**Table 3** Comparison of eigenfrequencies between reference model and Option 1

| Eigenfrequencies reference model [Hz] | Eigenfrequencies Option 1 [Hz] |
|---------------------------------------|--------------------------------|
| 2.4                                   | 1.8                            |
| 49.1                                  | 45.2                           |
| 61.2                                  | 59.1                           |
| –                                     | 97.8 (new)                     |
| 145.2                                 | 106.5                          |
| 203.9                                 | 206.1                          |
| 248.8                                 | 231.0                          |
| 311.6                                 | 311.6                          |

**Table 5** Comparison of eigenfrequencies between reference model and Option 3

| Eigenfrequencies reference model [Hz] | Eigenfrequencies Option 3 [Hz] |
|---------------------------------------|--------------------------------|
| 2.4                                   | 2.0                            |
| 49.1                                  | 48.5                           |
| 61.2                                  | 62.3                           |
| –                                     | 112.0 (new)                    |
| –                                     | 118.8 (new)                    |
| 145.2                                 | 151.8                          |
| 203.9                                 | 192.9                          |
| 248.8                                 | 237.7                          |
| 311.6                                 | 311.6                          |

**Table 7** Comparison of eigenfrequencies between reference model and Option 4

| Eigenfrequencies reference model [Hz] | Eigenfrequencies Option 4 [Hz] |
|---------------------------------------|--------------------------------|
| 2.4                                   | 1.9                            |
| 49.1                                  | 47.0                           |
| 61.2                                  | 63.0                           |
| 145.2                                 | 101.1                          |
| 203.9                                 | 180.6                          |
| 248.8                                 | 209.7                          |
| 311.6                                 | 311.3                          |

**Table 2** Comparison of eigenfrequencies between complex model and simplified model

| Eigenfrequencies complex model [Hz] | Eigenfrequencies simplified model [Hz] | Deviation [%] |
|-------------------------------------|--|---------------|
| 2.0                                 | 2.4                                    | +21           |
| 49.0                                | 49.1                                   | < +1          |
| 63.0                                | 61.2                                   | –3            |
| 145.7                               | 145.2                                  | < –1          |
| 196.9                               | 203.9                                  | +4            |
| 241.6                               | 248.8                                  | +3            |
| 311.6                               | 311.6                                  | 0             |

**Table 4** Comparison of eigenfrequencies between reference model and Option 2

| Eigenfrequencies reference model [Hz] | Eigenfrequencies Option 2 [Hz] |
|---------------------------------------|--------------------------------|
| 2.4                                   | 2.0                            |
| 49.1                                  | 48.9                           |
| 61.2                                  | 62.9                           |
| –                                     | 142.4 (new)                    |
| 145.2                                 | 145.7                          |
| 203.9                                 | 197.7                          |
| 248.8                                 | 240.9                          |
| 311.6                                 | 311.6                          |

**Table 6** Comparison of eigenfrequencies between reference model and Option 4

| Eigenfrequencies reference model [Hz] | Eigenfrequencies Option 4 [Hz] |
|---------------------------------------|--------------------------------|
| 2.4                                   | 2.0                            |
| 49.1                                  | 47.2                           |
| 61.2                                  | 63.0                           |
| 145.2                                 | 129.8                          |
| 203.9                                 | 186.6                          |
| 248.8                                 | 214.7                          |
| 311.6                                 | 311.3                          |

**Table 8** Comparison of eigenfrequencies between reference model and Option 5

| Eigenfrequencies reference model [Hz] | Eigenfrequencies Option 5 [Hz] |
|---------------------------------------|--------------------------------|
| 2.4                                   | 2.0                            |
| 49.1                                  | 48.4                           |
| 61.2                                  | 63.0                           |
| –                                     | 145.2 new                      |
| 145.2                                 | 145.8                          |
| 203.9                                 | 197.4                          |
| 248.8                                 | 243.5                          |
| 311.6                                 | 311.6                          |

**Fig. 11** Three-stepped gearbox with powertrain options investigated (Romax/NKE)

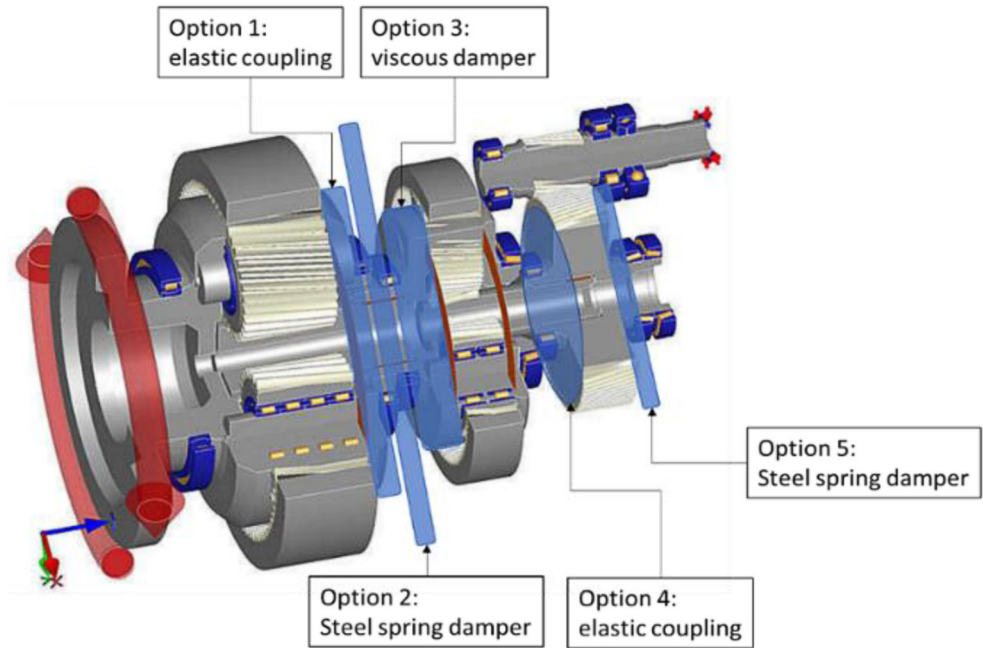
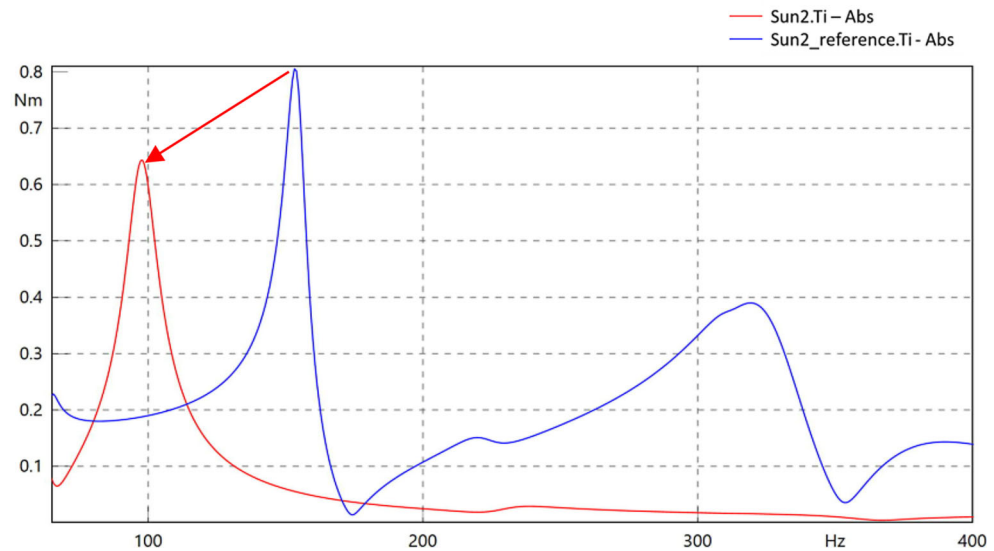


**Fig. 12** Frequency analysis—Option 2



highlighted in the model design (see Fig. 7). Based on the linearization of the system shown in Fig. 7 a frequency analysis is carried out. For this a harmonic input signal such as e.g. a sinusoidal curve is put into the system at both planet carriers to obtain the frequency response of this linearized system.

Figs. 12, 13, 14, 15 and 16 depict the results of the frequency analysis of sun2. The blue graph represents the system behavior of the reference model, whereas the red graph shows the effect of the option considered. The shift of eigenfrequencies of every option is shown in Tables 3, 4, 5, 6 and 7.

#### 4.1 Option 1—elastic coupling between the 1st and 2nd planetary stages

A drivetrain component which couples the planetary stages consequently, results in a comparatively massive coupling, transmitting the enormous static torque at this position by still allowing a certain torsional elasticity. The magnitude of mass moment of inertia added to the planetary carrier of the second stage leads to a comparatively high shift of natural frequencies. In this case the resonance is shifted from 145–98 Hz (see Table 3). The coupling’s outer diameter is 1700 mm and its mass approx. six tons.

**Fig. 13** Frequency analysis—Option 2

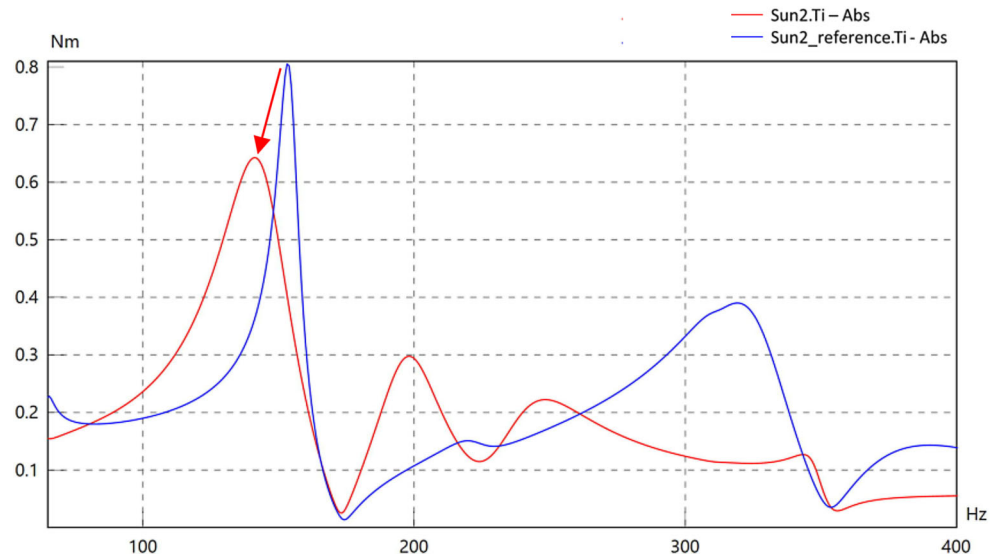
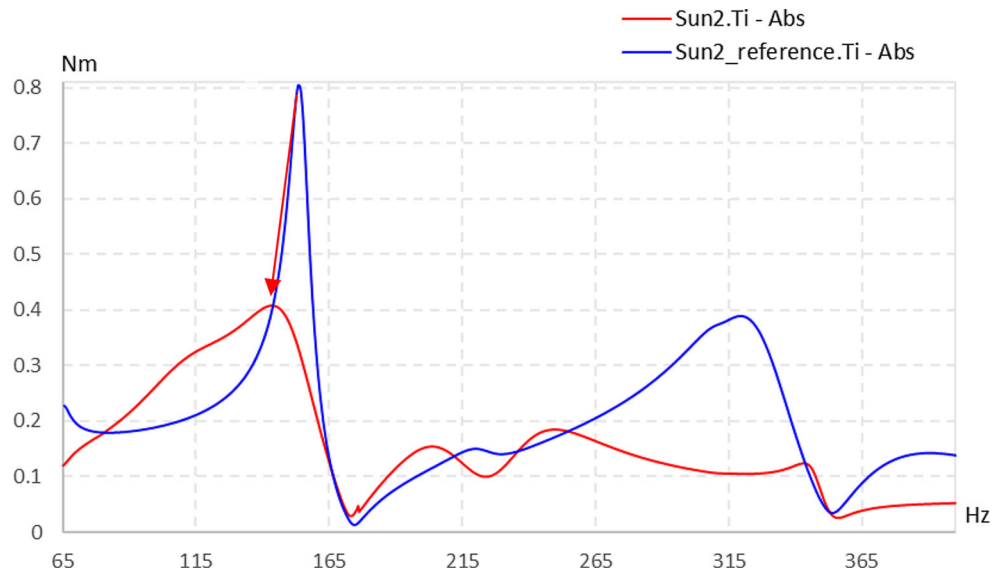


**Fig. 14** Frequency analysis—Option 3



The red graph in Fig. 12 indicates an amplitude reduction of approx. 22%. This is a result of the combination of relatively low torsional coupling stiffness and its effective friction and hydrodynamic damping. On the other hand, the resonance is shifted significantly to a lower frequency of slightly below 100 Hz. Thus, the resonance is shifted beyond the critical area.

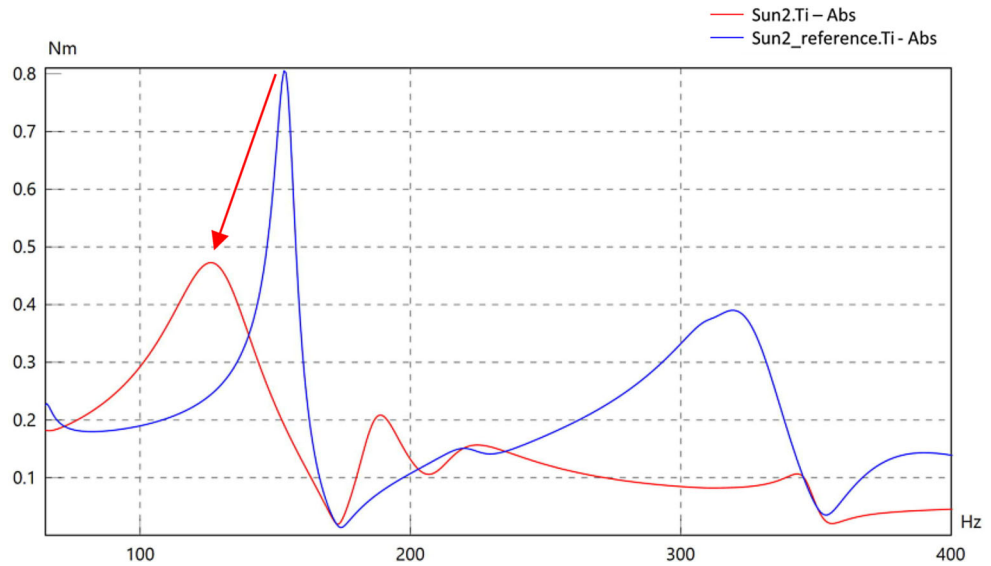
#### 4.2 Option 2—steel spring damper attached to 2nd planetary stage

For this investigation, the steel spring damper is attached to the 2nd planetary carrier, right between the first and second planetary stage. The damper's outer diameter is 1000 mm, its width 170 mm, and its mass approx. 800 kg. Table 4

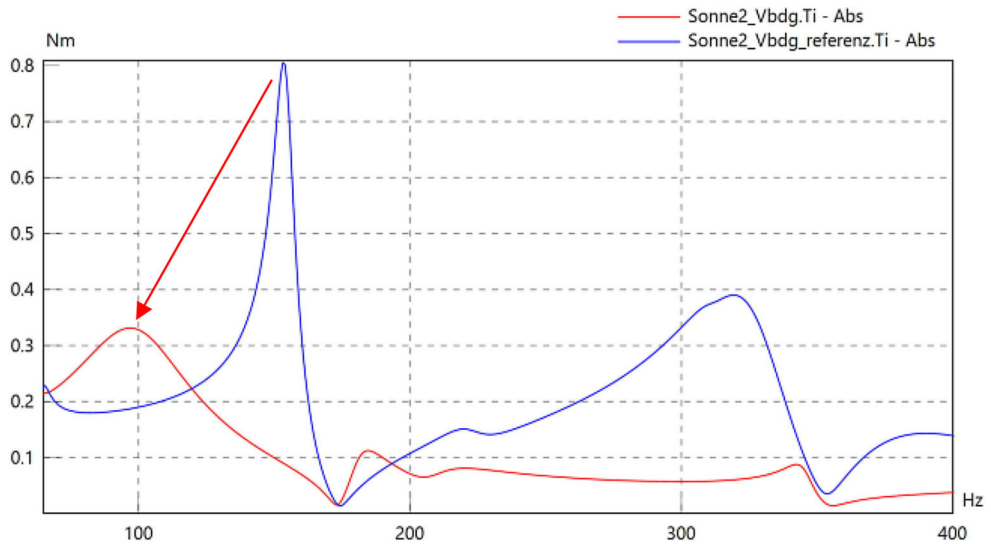
shows the comparison of the eigenfrequencies without and with a steel spring damper.

Fig. 13 clearly illustrates how the damper splits the main resonance at 145 Hz into two smaller amplitudes at 130 and 200 Hz. Normally, a significant stronger damping of the remaining amplitudes can be expected thanks to the effective friction and hydrodynamic-damping properties. Because of the required high torsional stiffness, which is necessary to tune the damper to the main resonance of 145 Hz (see Sect. 2.4), the damping effect is almost neglectable due to the low damper twist. In this configuration it reduces the amplitude by approx. 18%.

**Fig. 15** Frequency analysis—Option 4



**Fig. 16** Frequency analysis—Option 4



**4.3 Option 3—viscous damper attached to planet carrier 2nd stage**

Other than options 1 and 2, a viscous damper is attached directly to the planet carrier, utilizing the remaining space between the gearwheels and carrier. Such an integration causes only minor design implications to the gearbox. The viscous damper’s outer diameter is approx. 1700mm, its width 110mm, and its mass less than 700kg. The viscous damper features a special design with two separated inertia rings, allowing increased damping by maintaining low inertia. Additionally, inertia rings are not identical in order to achieve a better frequency tuning. Thus, the system shows two new natural frequencies instead of one (see Table 5).

The broadband damping effect effectively reduces the amplitude in the frequency band from 140 to 145Hz by approx. 50% (see Fig. 14).

**4.4 Option 4—gear integrated elastic coupling parallel stage**

The basic idea of integrating a coupling into the gearwheel of the 3rd stage (parallel stage) is derived from the proven solution of camshaft couplings in combustion engines to reduce engine noise (see Sect. 2.2). The coupling’s outer diameter is approx. 700mm (fitting to the design envelope of the gear wheel), and its mass approx. 400kg. Like option 1 the elastic coupling introduces torsional elasticity to the parallel stage and splits the torsional system into two tuned subsystems. This effect is depicted in Table 6 with a shift of the resonance from 145–130Hz.

The simulation result (see Fig. 15) depicts the shift of the natural frequencies and results in a reduction of the amplitude of approx. 40%, even if the coupling is not located directly at the source of excitation.

**Fig. 17** Frequency analysis—Option 4

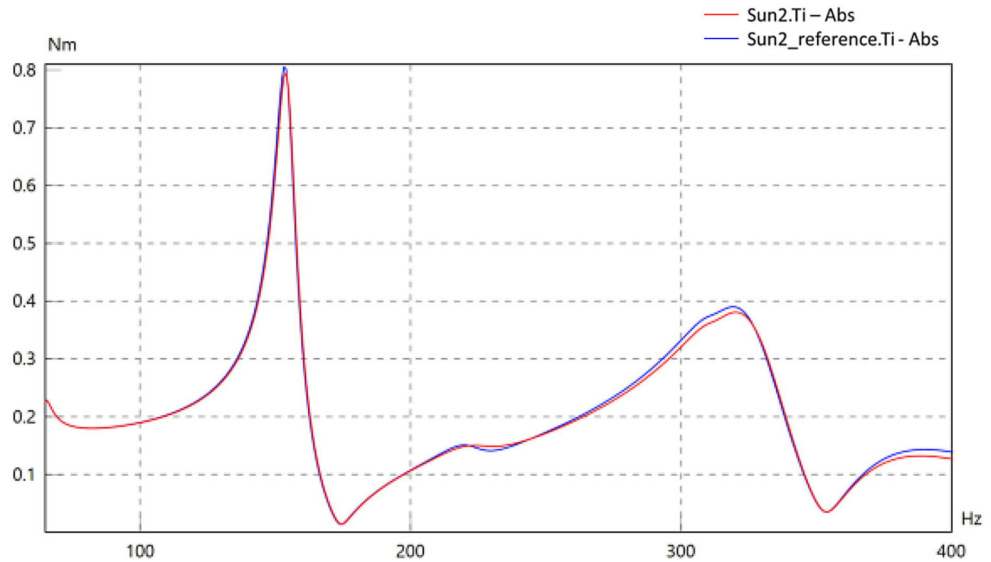
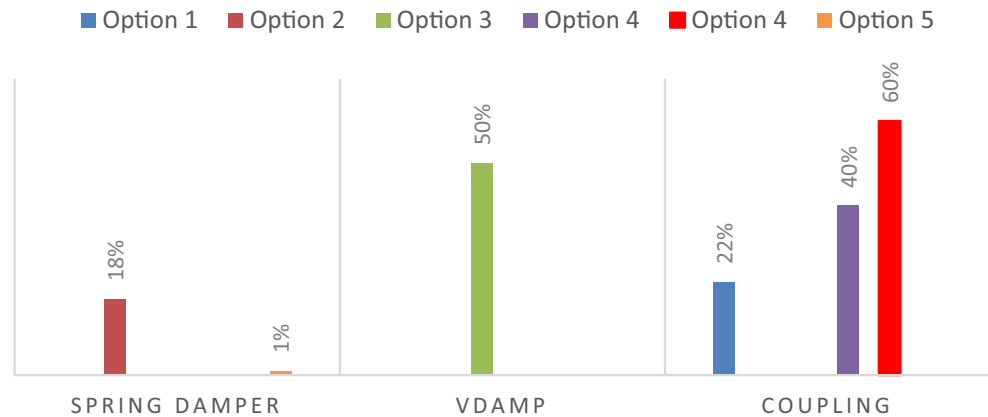


**Fig. 18** Summary of results. Resonance amplitude reduction of 145 Hz



A parameter study with increased torsional stiffness of the coupling reveals the importance of careful system tuning. Fig. 16 depicts a reduction of the amplitude by approx. 60%.

The eigenfrequencies for this case are displayed in Table 7.

#### 4.5 Option 5—steel spring damper attached to the parallel stage

In the fifth installation space a spring damper is installed right after the parallel gear (Table 8). This means that the damper is located far away from the position in which noise emissions arise. The damper's outer diameter is 630 mm, its width 102 mm, and its mass approx. 200 kg.

The results in Fig. 17 clearly show that the effect on the system is neglectable, the amplitude is reduced by less than 1% only.

## 5 Conclusion

Torsional dampers and torsional elastic couplings effectively shift natural frequencies and bear the potential to move resonances beyond critical areas. Translated to the application of internal combustion engines, that means that resonances are shifted effectively beyond critical speed range. For more than 60 years now, these products not only safeguard crank drives effectively but also prove their robustness and reliability even under harshest operating and environmental conditions.

The work of this paper shows that, powertrain components which have predominately been used for the reduction of torsional vibrations of combustion engines, bear a high potential to avoid wind turbine tonalities and to reduce the overall sound level of wind turbines. That can be important to meet future requirements on wind turbine noise, particularly with growing sizes of onshore wind turbines beyond the 5–6 MW class. Moreover, this technology bears the potential to create a competitive edge for wind turbine and

gearbox OE manufacturers: One specification for an entire platform could cope with all site-specific noise codes, also for big onshore turbines close to urbanized areas.

Comparing coupling Options 1 and 4 explains that the additional friction and hydrodynamic damping only is effective if the coupling stiffness allows a certain coupling twist to achieve sufficient damping of the remaining amplitudes.

Damper options 2 and 5 unveil a correlation between the distance of the damper from the source of excitations. The farther away the spring damper is located from the source of excitation, the less influence it has on the system. Regarding the magnitude of damping, the same applies for the couplings: The relative damper stiffness needs to allow a certain damper twist to achieve sufficient damping.

The broadband damping effect of the viscous damper not only reduces the main resonance at 145 Hz, but also leads to a reduction in resonances in the higher frequencies. In comparison to the spring damper Option 2 (planet carrier second stage), the viscous damper shows an advantage over the spring damper due to its flexibility in design. That allows better adjustment and fine-tuning of a viscous damper to meet the requirements on stiffness, damping and inertia, to achieve overall better performance.

Fig. 18 gives a brief overview on the effects of the various options.

The advantage of the integrability of such powertrain components into the gearbox is simultaneously posing a challenge which OEs and their system and component suppliers will have to accept: Tonality and sound remedies traditionally are taken after erecting a prototype and after

having performed measurements. The earlier in the development process a noise attenuating powertrain component will be considered, the more effective by a solution can be chosen and integrated. And finally, early stage consideration allows a higher degree of integration, resulting in a more cost-effective solution.

## References

1. Dawson BNM (2020) Tonal characteristics of wind turbine drive trains. Conference inter.noise 2014: <https://www.Acoust> Last Accessed 11:12
2. Wind Power ZF (2020) Leading wind turbine gearbox technology in noise reduction. Think Tank in PES Wind 2/18: <https://www.Pesucum.com/wind/leading-wind-turbine-gearbox-technology-in-noise-reduction/> Last Accessed 11:12
3. Prenninger K (2017) S. Lange , D. Richter-Trummer, EFFECTS OF ENGINE AND VESSEL OPERATING CONDITIONS ON TORSIONAL VIBRATION DAMPERS, Torsional Vibrations Symposium. Geislinger GmbH, Salzburg
4. Zengxin Gao, Kari Saine, Sami Oksanen: SOLAS new noise regulation impact on engine noise reduction and engine room, Proceedings of the 28th CIMAC Congress, Helsinki (2016)
5. Geislinger GmbH Homepage, <http://www.geislinger.com>, Accessed 14 Nov 2020
6. Hafner KE, Maas H (1985) Berlin: VEB Verlag Technik. Torsionsschwingungen in der Verbrennungskraftmaschine, vol 4. Springer, Wien
7. Mühlberger C (2017) K. Prenninger, J. Krah, M. Geislinger, INFLUENCE OF DAMPING FACTORS ON COUPLING APPLICATIONS, Torsional Vibrations. Symposium, Salzburg
8. Dresig H, Fidlín A (2020) Schwingungen mechanischer Antriebssysteme, 4th edn. Springer, Berlin Heidelberg
9. Berichte Nr VDI (2019) 2346, 10. VDI, Fachtung Schwingung von Windenergieanlagen

## Terms and Conditions

Springer Nature journal content, brought to you courtesy of Springer Nature Customer Service Center GmbH (“Springer Nature”).

Springer Nature supports a reasonable amount of sharing of research papers by authors, subscribers and authorised users (“Users”), for small-scale personal, non-commercial use provided that all copyright, trade and service marks and other proprietary notices are maintained. By accessing, sharing, receiving or otherwise using the Springer Nature journal content you agree to these terms of use (“Terms”). For these purposes, Springer Nature considers academic use (by researchers and students) to be non-commercial.

These Terms are supplementary and will apply in addition to any applicable website terms and conditions, a relevant site licence or a personal subscription. These Terms will prevail over any conflict or ambiguity with regards to the relevant terms, a site licence or a personal subscription (to the extent of the conflict or ambiguity only). For Creative Commons-licensed articles, the terms of the Creative Commons license used will apply.

We collect and use personal data to provide access to the Springer Nature journal content. We may also use these personal data internally within ResearchGate and Springer Nature and as agreed share it, in an anonymised way, for purposes of tracking, analysis and reporting. We will not otherwise disclose your personal data outside the ResearchGate or the Springer Nature group of companies unless we have your permission as detailed in the Privacy Policy.

While Users may use the Springer Nature journal content for small scale, personal non-commercial use, it is important to note that Users may not:

1. use such content for the purpose of providing other users with access on a regular or large scale basis or as a means to circumvent access control;
2. use such content where to do so would be considered a criminal or statutory offence in any jurisdiction, or gives rise to civil liability, or is otherwise unlawful;
3. falsely or misleadingly imply or suggest endorsement, approval, sponsorship, or association unless explicitly agreed to by Springer Nature in writing;
4. use bots or other automated methods to access the content or redirect messages
5. override any security feature or exclusionary protocol; or
6. share the content in order to create substitute for Springer Nature products or services or a systematic database of Springer Nature journal content.

In line with the restriction against commercial use, Springer Nature does not permit the creation of a product or service that creates revenue, royalties, rent or income from our content or its inclusion as part of a paid for service or for other commercial gain. Springer Nature journal content cannot be used for inter-library loans and librarians may not upload Springer Nature journal content on a large scale into their, or any other, institutional repository.

These terms of use are reviewed regularly and may be amended at any time. Springer Nature is not obligated to publish any information or content on this website and may remove it or features or functionality at our sole discretion, at any time with or without notice. Springer Nature may revoke this licence to you at any time and remove access to any copies of the Springer Nature journal content which have been saved.

To the fullest extent permitted by law, Springer Nature makes no warranties, representations or guarantees to Users, either express or implied with respect to the Springer nature journal content and all parties disclaim and waive any implied warranties or warranties imposed by law, including merchantability or fitness for any particular purpose.

Please note that these rights do not automatically extend to content, data or other material published by Springer Nature that may be licensed from third parties.

If you would like to use or distribute our Springer Nature journal content to a wider audience or on a regular basis or in any other manner not expressly permitted by these Terms, please contact Springer Nature at

[onlineservice@springernature.com](mailto:onlineservice@springernature.com)